

## Analysis of the 213-MeV Proton-Proton Scattering Data\*

PETER SIGNELL, N. R. YODER, AND J. E. MATOS

*Physics Department, The Pennsylvania State University, University Park, Pennsylvania*

(Received 13 April 1964)

Modified phase-shift analyses have been made of the 213-MeV Rochester data, with a statistical argument used to eliminate three of the data. The methods of obtaining the least-squares fit to the data, and of choosing the phase shifts to be searched upon are examined in some detail. Thirteen free phases are preferred and most of these are found to have very small uncertainties. Several of the data subgroups give unexpectedly low contributions to  $\chi^2$ , but are still influential in limiting the phase-shift standard deviations. All models so far proposed for the proton-proton interaction give poorer fit to the data by an order of magnitude than does the modified phase analysis. The solution of the type 2 of Stapp, Ypsilantis, and Metropolis has a  $\chi^2$  probability of less than 1%. The pion-nucleon coupling constant could only be roughly evaluated, giving qualitative evidence for the one pion exchange mechanism. Estimates have been made of the effectiveness of several possible extensions of the measurements.

### I. INTRODUCTION

A NUMBER of very precise proton-proton scattering experiments have recently been completed at the Rochester Synchrocyclotron Laboratory. Single, double, and triple scattering data have been taken from 30 to 90° c.m. in the vicinity of 210 MeV (incident energy in the laboratory).

Preliminary "modified phase-shift analyses" of some of the present data have been reported<sup>1</sup> by MacGregor *et al.* and by the present authors. An encouraging finding reported by our group was that the phase-shift uncertainties were much reduced from earlier estimates<sup>1</sup> of Breit *et al.* The present communication reports our completed analysis in detail.

### II. DATA SELECTION

All of the 43 data considered for this analysis are shown in Table I. The experimental unpolarized cross section was unnormalized, so an absolute value of  $\sigma(90^\circ)$  was obtained by interpolation as in Fig. 1. Note that the standard deviation obtained was substantially smaller than that obtained by Konradi<sup>2,3</sup> from an interpolation. The 210-MeV polarization measurements  $P(\theta)$  were used as though measured at 213 MeV. This is certainly a negligible source of error since  $P(\theta)$  varies only slowly with energy in this energy region and angular range.<sup>4</sup> The  $P(90^\circ)$  datum was not used since it would falsely increase the number of degrees of freedom. Preliminary "modified phase-shift analyses"<sup>5</sup> were made with 13, and then 20, low angular momentum ( $L$ ) phases

adjusted so as to produce a least-squares fit to the data. The higher phases were set equal to their one-pion-exchange (OPE) values.<sup>5</sup> The four data which had the largest contributions to the least-squares error sum  $\chi^2$  are shown in Table II. Comparing the first and seventh lines, and the second and eighth, one sees that 7% of the data accounts for 65% of the  $\chi^2$ , even when the number of "free" phases is at the absurd value of twenty. These three data, then, are inconsistent with the rest of the data when combined with the invariance requirements of the phase-shift analysis. Those data should certainly be deleted from the set.

However, one has still to decide how much of a deviation from the mean will be tolerated. One method is to compute that deviation for which the data set at hand has a probability of  $\frac{1}{2}$  of containing such a datum. For

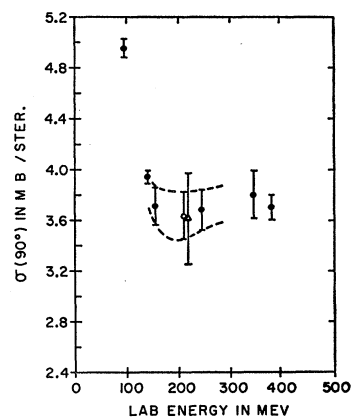


FIG. 1.  $\sigma(90^\circ)$  versus energy. The solid circles and errors were obtained by quadratically combining the data in the angular regions and at the energies: 62–112°, 156 MeV, C. Caversazio, K. Kuroda, and A. Michaelowicz, *J. Phys. Radium* **22**, 628 (1961); 60–90°, 240 and 250 MeV, W. N. Hess, *Rev. Mod. Phys.* **30**, 368 (1958); 80–89°, 345 MeV, O. Chamberlain, E. Segrè, and C. Wiegand, *Phys. Rev.* **83**, 923 (1951); 90°, 380 MeV, J. Holt, J. Kluyver, and J. Moore, *Proc. Phys. Soc. (London)* **71**, 781 (1958). The points at 142 and 96.5 MeV were from phase-shift analyses reported by one of us (P.S.S.) in *Phys. Rev.* **133**, B982 (1964). See also Ref. 3, p. 79. The open circle is our interpolated datum; the triangle is Konradi's, Ref. 2.

\* Supported in part by the U. S. Atomic Energy Commission.

<sup>1</sup> K. Gotow, F. Lobkowicz, and E. Heer, *Phys. Rev.* **127**, 2206 (1962), see especially p. 2215.

<sup>2</sup> A. Konradi, thesis, University of Rochester, 1961 (unpublished). Quoted as a normalization error in Ref. 3, p. 186.

<sup>3</sup> R. Wilson, *The Nucleon-Nucleon Interaction* (Interscience Publishers, Inc., New York, 1963).

<sup>4</sup> See Figs. 5 and 6, p. 81 of Ref. 3.

<sup>5</sup> M. J. Moravcsik, University of California Radiation Lab. Report, UCRL 5317-T, 1958 (unpublished); P. Cziffra, M. H. MacGregor, M. J. Moravcsik, and H. P. Stapp, *Phys. Rev.* **114**, 880 (1959).

TABLE I. Data considered for analysis.  $N_p$  indicates (absolute) normalization for the relative values which follow. The cross section is relative only (see text). The spin precession angle is indicated by  $\chi$ . "upao" means "used in preliminary analyses only."

Experimental energy (MeV)	c. m. Angle (deg)	Type	Parameter	Error	$\chi$ (deg)	Reference	Remarks
210.	30.	$N_p$	1.000	0.022		a	
		$P$	0.312	0.006			
	40.		0.319	0.0085			
			0.303	0.0075			
			0.240	0.006			
			0.163	0.007			
80.		0.084	0.007				
		0.084	0.007				
213.	90.		3.63	0.20	b	Interpolated	
213.	30.	$\sigma_{abs}$	3.800	0.053	c		
		$\sigma_{rel}$	3.833	0.046			
	40.		3.740	0.041			
			3.648	0.038			
	60.		3.665	0.035			
			3.662	0.031			
	80.		3.615	0.035			
			3.615	0.035			
213.	30.	$D$	0.200	0.016	d		
			0.232	0.026			
	40.		0.240	0.018			
			0.319	0.021			
	60.		0.297	0.030			
			0.360	0.070			
213.	30.	$R$	-0.203	0.012	e		
			-0.133	0.017			
	40.		-0.041	0.018			
			0.071	0.026			
	60.		0.147	0.029			
			0.248	0.042			
213.	30.	$AR$	-0.449	0.016	e	63.3	
			-0.343	0.015			
	40.		-0.202	0.017			
			-0.059	0.018			
	60.		0.053	0.029			
			0.032	0.036			
213.	30.	$R'R$	-0.060	0.064	f	63.3	
			0.331	0.021			
	40.		0.277	0.019			
			0.135	0.017			
	60.		0.070	0.018			
			-0.313	0.036			
80.		-0.307	0.053	121.9			
		-0.406	0.082		122.8		
						upao	
							upao

<sup>a</sup> J. H. Tinlot and R. E. Warner, Phys. Rev. **124**, 890 (1961). Note that absolute errors for  $P(\theta)$  are erroneously listed as relative in Ref. 3, p. 200.

<sup>b</sup> Interpolated as in Fig. 1.

<sup>c</sup> A. Konradi; thesis, University of Rochester, 1961 (unpublished).

<sup>d</sup> See Ref. 1.

<sup>e</sup> A. England, W. Gibson, K. Gotow, E. Heer, and J. Tinlot, Phys. Rev. **124**, 561 (1961).  $AR = A \sin \chi + R \cos \chi$ .

<sup>f</sup> F. Lobkowicz and K. Gotow (private communication).  $R'R = R' \sin \chi + R \cos \chi$ .

TABLE II. The four data with the largest contribution to  $\chi^2$ . The number of data is indicated by  $N_D$ , the number of searched-upon phases by  $N$ . The  $\chi^2$  ratio is  $\chi^2$  divided by its expected value.

$N_D$	$N$	$\chi^2$	$\chi^2$ Ratio	Contributions to $\chi^2$			
				$R'R(60^\circ)$	$R'R(70^\circ)$	$AR(80^\circ)$	$AR(90^\circ)$
43	13	64.2	2.14	10.8	16.1	5.6	11.6
43	20	57.9	2.52	9.8	13.2	4.6	10.2
42	13	52.1	1.80	11.5	14.4	6.1	
42	20	46.8	2.13	9.3	13.0	5.8	
41	13	34.0	1.22			4.5	10.6
41	20	28.7	1.37			2.8	9.3
40	13	22.8	0.85			5.0	
40	20	18.7	0.93			3.8	

43 data, this corresponds to 2.5 standard deviations.<sup>6</sup> Thus, by this criterion there should be "no" datum in our set which is more than 2.5 standard deviations from the mean. If there are such data, and if those who measured the data do not wish to withdraw them or alter the experimental errors, then one should withdraw those data on statistical grounds. That was the case here, after careful consideration of the analysis results by the Rochester group.<sup>7</sup> For the rest of the analyses, then, the  $AR(90^\circ)$ ,  $R'R(60^\circ)$ , and  $R'R(70^\circ)$  were omitted. The  $AR(80^\circ)$  was retained, since it is statistically plausible that one of the forty remaining data would be about two standard deviations from the mean.<sup>6</sup>

We note that the above argument for rejecting individual data would break down if a data subgroup [ $AR(\theta)$ , say] drifted to ever larger deviations from the mean with increasing angle. In that case, one would tend to discard the entire data subgroup which showed the trend. It is possible that the  $AR(80^\circ)$  and  $AR(90^\circ)$  show such a trend away from the mean (Fig. 7), but certainly  $AR(70^\circ)$  does not. It is difficult to establish a trend on the basis of two data, so we have preferred to retain  $AR(80^\circ)$ . The sensitivity of the analysis to retention of  $AR(80^\circ)$  will be examined in Sec. VI. In any case, experiments now under way<sup>7</sup> to measure  $AR(80-120^\circ)$  with improved accuracy should clear up the discrepancy.

### III. METHODOLOGY

The general method and notation have been described in a previous communication.<sup>8</sup> It may be of some use, however, to have an elaboration of several of the techniques.

#### A. Minimization Technique

The technique used for the minimization of the least-squares error sum  $q(x^2)$  was developed by us and also by a group at ORNL.<sup>9</sup>

In order to use the usual statistical formulas,  $q$  must be fairly accurately quadratic in the space of the searched-upon parameters, out to the surface for which  $q$  is greater by unity than its value at the minimum. If one is sufficiently close to the minimum, it is a good approximation to assume that  $q$  is at most a quadratic function of the searched-upon parameters  $x_i$ :

$$q(x) = q(x_0) + \mathbf{G}(x_0) \cdot (\mathbf{x} - \mathbf{x}_0) + \frac{1}{2} (\mathbf{x} - \mathbf{x}_0) \cdot S \cdot (\mathbf{x} - \mathbf{x}_0),$$

where  $S$  is dyadic and  $\mathbf{G}$  and  $\mathbf{x}$  are vectorial. With  $\mathbf{x}_0$  the

point of minimum in  $q$ ,  $\mathbf{G}(x_0) = 0$  and  $\mathbf{G}(x) \equiv \nabla q(x) = S \cdot (\mathbf{x} - \mathbf{x}_0)$ . Solving,  $\Delta \equiv \mathbf{x} - \mathbf{x}_0 = S^{-1} \cdot \mathbf{G}(x)$ . Thus, in order to find the vector from an arbitrary starting point to the minimum, one needs the first and second derivatives,  $\mathbf{G}$  and  $S$ , of  $q$  with respect to the  $x_i$ .

The second derivatives  $S_{ij} \equiv \partial^2 q / \partial x_i \partial x_j$  usually involve lengthy computations. A useful approximation can be obtained by taking the derivatives inside the summation in the definition of  $q$ .<sup>10</sup>

$$q \equiv \sum_n \{ [p_n(x) - d_n] / \epsilon_n \}^2.$$

Here,  $p_n(x)$  is the predicted value for an experimental datum  $d_n$  with experimental standard deviation  $\epsilon_n$ . Then, with

$$g_{ni} \equiv \partial p_n / \partial x_i \quad \text{and} \quad s_{nij} \equiv \partial^2 p_n / \partial x_i \partial x_j,$$

$$G_i = 2 \sum_n \frac{p_n - d_n}{\epsilon_n^2} g_{ni},$$

and

$$S_{ij} = 2 \sum_n \frac{g_{ni} g_{nj}}{\epsilon_n^2} + 2 \sum_n \frac{p_n(x) - d_n}{\epsilon_n^2} s_{nij}.$$

In the vicinity of a minimum in  $q$ , the last term above tends to zero. We refer to  $S$  without it as the "linearized" second derivative. The problem is thus reduced to constructing the  $\mathbf{G}$  and  $S$  from the  $g_{ni}$ ; the desired vector to the minimum is immediate.

In general, one starts out at some position  $\mathbf{x}$  which does not correspond to a minimum, so the  $q$  is only approximately quadratic and the predicted  $\Delta$  is only an approximation. By repetition of the process, however, one approaches the minimum if the initial guess  $\mathbf{x}$  is sufficiently close to  $\mathbf{x}_0$ . The method obviously accelerates as it approaches a minimum.

When actually using the method, the iterations were stopped when the  $q$  ceased decreasing. It was assumed that one was sufficiently close to the minimum if the final  $\Delta_i$  were at least an order of magnitude less than the standard deviations  $\sigma_i$  on the predicted  $x_i$ . A typical iteration series is shown in Table III. The solution  $\mathbf{x}_0$  was found to be independent of the starting point  $\mathbf{x}$  providing the latter was varied in the domain of the same gross solution. This is as it should be for a good minimization technique.

Comparison iteration series were made with the same starting points, but without the linearizing assumption. The two methods always converged to the same solution in the same number of iterations. For actual analyses of the 213-MeV data, the linearized version required about one-seventh the computation time of the full version.

An added advantage of the "quadratic" minimization methods is that the  $\sigma_i$ , the standard deviations on the  $x_i$ ,

<sup>6</sup> See, for instance, C. D. Hodgmann, *Mathematical Tables* (Chemical Rubber Publishing Company, Cleveland, 1947), p. 203-208.

<sup>7</sup> K. Gotow and F. Lobkowitz (private communication).

<sup>8</sup> P. Signell, N. R. Yoder, and N. M. Miskovsky, *Phys. Rev.* **133**, B1490 (1964).

<sup>9</sup> M. H. Lietzke, Oak Ridge Report ORNL-3259, 1962 (unpublished), which is the description of a FORTRAN computer program.

<sup>10</sup> P. Cziffra and M. J. Moravcsik, University of California Radiation Laboratory Report, UCRL-8523 Rev., 1959 (unpublished).

TABLE III. Sample of a search for a minimum in  $\chi^2$ . The search is for  $N=6$ ,  $g^2=14.4$  (fixed), solution No. 1, 40-piece data set, with the  ${}^3F_2$  phase being tried as the sixth released phase (see text, Sec. IIIB). The  ${}^3P_1$ ,  ${}^3P_2$ , and  ${}^1D_2$  phases are not shown. Their (initial, final) nuclear bar values in degrees were  $(-22.04, -29.04)$ ,  $(16.06, 17.82)$ ,  $(7.20, 8.44)$ , respectively. The nuclear bar phase shifts, in degrees, are denoted by  $\delta$ , the estimated distance to the  $\chi^2$  minimum by  $\Delta$ , and the estimated standard deviation by  $\sigma$ . The number of iterations shown exceeds that necessary. The entire process takes about 30 seconds on an IBM 7094.

Iteration No.	$\chi^2$	${}^1S_0$			${}^3P_0$			${}^3F_2$		
		$\delta_0$	$\Delta_0$	$\sigma_0$	$\delta_{10}$	$\Delta_{10}$	$\sigma_{10}$	$\delta_{32}$	$\Delta_{32}$	$\sigma_{32}$
0	1320.	5.298	2.217	2.09	-1.261	1.627	2.13	2.154	-2.674	0.90
1	365.	7.515	-0.240	1.37	0.367	-1.086	1.52	-0.520	-0.329	0.57
2	344.7	7.275	0.053	1.31	-0.719	-0.160	1.49	-0.849	-0.034	0.56
3	344.31	7.328	0.001	1.31	-0.879	-0.021	1.49	-0.884	-0.004	0.56
4	344.3015	7.329	0.001	1.31	-0.900	-0.003	1.49	-0.887	-0.001	0.56
5	344.3013	7.330			-0.903			-0.888		

are trivially obtainable from the second-derivative matrix  $S$ .

It was mentioned at the beginning of this section that  $q(\chi^2)$  must be fairly accurately quadratic out to where it is greater by unity than its value at the minimum. It was found that  $q$  was indeed sufficiently quadratic to delineate the standard deviations to the desired accuracy for the analyses reported here.

### B. Phase-Shift Ordering

The order in which the low- $L$  phase shifts are released from the OPE (or other model) values should be that for which  $\chi^2$  is made a minimum at each number  $N$  of searched-upon phases. A methodical way of ordering the phases was devised, in an attempt to meet the above criterion and in order to obtain  $F$  probabilities.<sup>10</sup>

At 213 MeV, the  $L \leq 2$  phases are surely not at their OPE values, so one has at least six free phases:  ${}^1S_0$ ,  ${}^3P_{0,1,2}$ ,  $\epsilon_2$ , and  ${}^1D_2$ . The higher  $L$  phases were tried in turn as the seventh free phase, except that no phase was released before a similar one two units of angular momentum below it. Of the five candidates thus tried for the seventh released phase, the one yielding the lowest minimized  $\chi^2$  was chosen. One might argue that all  $L=3$  phases should be released together, and before any for which  $L \geq 4$ . Yet the OPE phases with  $L=J-1$  are anomalously small,<sup>11</sup> so perhaps should be released earlier. Again, spin and isospin matrix elements can overwhelm the centrifugal barrier differences between triplet  $L$  and singlet  $L \pm 1$ . We thus only use the centrifugal barrier argument to order phases with the same  $L$ -to- $J$  relationship.

Details of the ordering procedure are shown in Table IV for a portion of a typical analysis. The procedure was carried out by an automatic computer program which also computed the  $\chi^2$  and  $F$  probabilities.

### IV. RESULTS OF THE MODIFIED ANALYSES

The order in which the phases were released, following the procedure outlined in Sec. IIIB, is shown in Table V.

<sup>11</sup> For instance, their threshold behavior is  $\delta_l \sim k^{2l+3}$  rather than the usual  $k^{2l+1}$ .

TABLE IV. Sample of phase-shift ordering (see text, Sec. IIIB), for the same case as Table III. The  ${}^3F_4$  was finally chosen as the sixth released phase,  $\epsilon_2$  as the seventh.

Candidate for 6th phase	${}^3F_2$	${}^3F_3$	${}^3F_4$	$\epsilon_2$	${}^1G_4$
Minimized $\chi^2$	344	510	206	436	600
Candidate for 7th phase	${}^3F_2$	${}^3F_3$	${}^3H_6$	$\epsilon_2$	${}^1G_4$
Minimized $\chi^2$	205	206	206	67	186

Although the solution labeled  $N=16$  has the lowest  $\chi^2$  ratio, hence the highest  $\chi^2$  probability  $P_q$ , the latter does not vary significantly in the range  $N=14$  to 19. Thus, the  $\chi^2$  test<sup>10</sup> does not choose between the solutions in that range. The  $F$  probability, however, changes drastically, with jumps between  $N=14, 15$  and 16, 17. Specifically, the  $F$  test states that one has a 15% statistical probability of being correct in taking the fifteenth phase at its OPE value, 61% in taking the seventeenth at OPE.

The  $L=J$  phases for solutions  $N=13-16$  are examined in Table VI. Generally, the free phases are

TABLE V. Results of the modified phase analyses with  $g^2=14.4$ .  $N$  is the number of free (searched-upon) phases.  $M$  is the expected value of  $\chi^2$  (the number of degrees of freedom), and the  $\chi^2$  ratio is  $\chi^2/M$ . The phase shift shown is the one finally chosen to be released at that  $N$ .  $P_F$  is the probability that  $F$  is larger,  $P_q$  the probability that  $\chi^2$  is higher.

$N$	Phase	$\chi^2$	$M$	$\chi^2$ Ratio	$P_q$	$P_F$
5	${}^1D_2$	631.	35	18.		
6	${}^3F_4$	206.	34	6.1		
7	$\epsilon_2$	66.8	33	2.0	0.00	
8	${}^3F_3$	47.2	32	1.48	0.04	
9	${}^1G_4$	36.1	31	1.16	0.25	0.00
10	${}^3H_6$	30.6	30	1.02	0.44	0.02
11	$\epsilon_4$	28.1	29	0.968	0.52	0.10
12	${}^3F_2$	24.7	28	0.884	0.65	0.05
13	${}^3H_5$	22.8	27	0.844	0.70	0.13
14	${}^3K_7$	18.7	26	0.721	0.85	0.02
15	$\epsilon_6$	17.3	25	0.693	0.87	0.15
16	${}^3M_9$	16.0	24	0.665	0.89	0.15
17	${}^3H_4$	15.8	23	0.686	0.86	0.61
18	${}^3K_5$	15.4	22	0.701	0.84	0.48
19	${}^3K_3$	14.7	21	0.702	0.83	0.32
20	$\epsilon_8$	14.6	20	0.730	0.80	0.66
21	${}^3M_8$	14.4	19	0.759	0.76	0.62

TABLE VI. The  $L=J$  phases corresponding to Table V. The values are nuclear bar, in degrees.

$N$	${}^3P_1$	${}^3F_3$	${}^3H_5$	${}^3K_7$	${}^3M_9$
13	$-22.09 \pm 0.71$	$-2.62 \pm 0.21$	$-0.64 \pm 0.18$		
14	$-22.38 \pm 0.67$	$-3.10 \pm 0.28$	$-0.90 \pm 0.21$	$-0.65 \pm 0.16$	
16	$-22.30 \pm 0.66$	$-2.87 \pm 0.34$	$-0.59 \pm 0.31$	$-0.55 \pm 0.19$	$0.04 \pm 0.11$
OPE	$-30.30$	$-3.66$	$-0.93$	$-0.29$	$-0.10$
HJ	$-20.94$	$-2.85$	$-0.75$	$-0.24$	
Yale	$-21.79$	$-3.48$	$-1.04$	$-0.32$	

smaller than their OPEC values for  $L=1, 3, 5$ . For  $L=7$ , however, they are considerably larger. In contrast, the Hamada-Johnston<sup>12</sup> and Yale<sup>13</sup> potential  $L=J=7$  phases show only a small departure from OPEC. We regard the large departure of  ${}^3K_7$  from OPE as *unphysical*, probably due to some combination of fluctuations in the data. Our conclusion is that  $N=13$  is probably the best solution to use. We note, however, that Table VI indicates a greater uncertainty for the  ${}^3H_5$  phase than its standard deviation would indicate.

It is interesting that the  $L=J-1$  phases  ${}^3F_4$  and  ${}^3H_6$  are released earlier than the other phases of like  $L$  (see Table VI). This is as one would expect from the discussion at the end of Sec. III B. Also note that the  $L=J+1$  phases  ${}^3F_2$  and  ${}^3H_4$  are released last. If there were perfect uniformity in the order of release, one might expect that each phase would be released at a value of  $N$  which is five higher than that for which the phase two units of angular momentum lower was released. Thus, if  ${}^3F_3$  was the eighth released phase,  ${}^3H_5$  would be the thirteenth. Table VII shows that, although the phases were released in a somewhat strange order

among like  $L$ , there is still a very strong pattern of the kind just described. One sees that the fourteenth phase should have been  ${}^1I_6$  or  ${}^3K_8$ , and certainly *not*  ${}^3K_7$ , which should have been eighteenth or so. We take this to be further evidence for stopping at thirteen phases despite the very low 2%  $F$  probability.

TABLE VII. Comparison of values of  $N$ , the number of searched-upon phases, for the release of phases with the same  $L$ -to- $J$  relationship.

Phase	$N(\delta_{LJ})$	$N(\delta_{LJ}) - N(\delta_{L-2, J-2})$
${}^1G_4$	9	5
$\epsilon_4$	11	4
${}^3H_4$	17	5
${}^3H_5$	13	5
${}^3H_6$	10	4
$\epsilon_6$	15	4

From the foregoing discussion and examination of Table V, the  $F$  test would seem to favor  $N=16$  and 19. The phases for these, and for our physically favored  $N=13$ , are shown in Table VIII. As expected from the only gradual decrease of  $\chi^2$  with  $N$  in Table V, the higher  $L$  phases do not go to values wildly different from OPE.

The predicted values of the experimental quantities

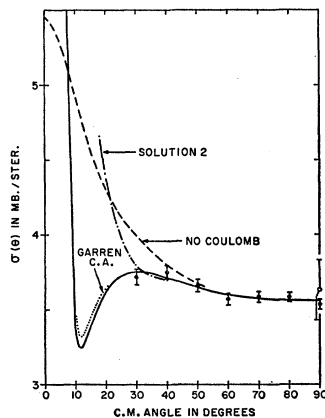


FIG. 2. The unpolarized cross-section data, normalized by  $N_p=0.978$  from the  $N=13$  analysis. The solid line is the prediction of the  $N=13$  analysis with the ordinary Coulomb amplitude. The dashed line is the same solution but with the proton charge set equal to zero. The dotted line is for the Garren amplitude (Ref. 19) substituted for the Coulomb amplitude and  $\chi^2$  reminimized. The dash-dot line is the solution 2 prediction, multiplied by the quotient of the normalizations for the two solutions. For solution 2,  $N_p=1.041$ .

<sup>12</sup> T. Hamada and I. D. Johnston, Nucl. Phys. **34**, 382 (1962).  
<sup>13</sup> K. E. Lassila, M. H. Hull, Jr., H. M. Ruppel, F. A. McDonald, and G. Breit, Phys. Rev. **126**, 881 (1962).

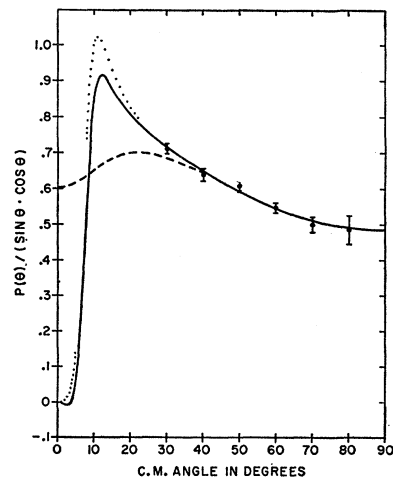


FIG. 3. The polarization data, divided by  $(\sin\theta \cos\theta)$  and normalized by  $N_p=0.985$ . Notation as in Fig. 2. Note the larger interference maximum with the Garren amplitude, and the better-than-expected fit of the solid line to the data.

TABLE VIII. The nuclear bar phase shifts, in degrees, from several of the analyses of Table V. A number in parenthesis is the *N* value at which the associated phase was released from its OPE value.

<i>N</i>	$^1S_0$	$^3P_0$	$^3P_1$	$^3P_2$	$\epsilon_2(7)$
13	5.19±0.44	-1.37±0.58	-22.09±0.71	15.99±0.28	-2.85±0.19
16	4.71±0.52	-1.72±0.57	-22.30±0.66	15.98±0.39	-3.06±0.23
19	4.54±0.55	-1.34±0.79	-21.85±0.84	16.44±0.61	-3.01±0.26
OPE					-5.37
	$^1D_2(5)$	$^3F_2(12)$	$^3F_3(8)$	$^3F_4(6)$	$\epsilon_4(11)$
13	7.13±0.29	1.49±0.37	-2.62±0.21	2.25±0.20	-1.03±0.09
16	7.08±0.36	1.33±0.40	-2.87±0.34	2.09±0.27	-1.15±0.10
19	6.93±0.40	1.86±0.58	-2.55±0.52	2.51±0.47	-1.15±0.10
OPE	2.26	2.13	-3.62	0.64	-1.24
	$^1G_{14}(9)$	$^3H_4(17)$	$^3H_5(13)$	$^3H_6(10)$	$\epsilon_6(15)$
13	1.12±0.14		-0.64±0.18	0.35±0.09	
16	0.93±0.19		-0.59±0.31	0.30±0.11	-0.50±0.07
19	0.89±0.21	0.68±0.37	-0.39±0.36	0.57±0.33	-0.46±0.09
OPE	0.74	0.36	-0.91	0.15	-0.38
	$^1I_6$	$^3K_6(18)$	$^3K_7(14)$	$^3K_8(19)$	$\epsilon_8$
16			-0.55±0.19		
19		0.46±0.35	-0.45±0.24	0.30±0.29	
OPE	0.27	0.09	-0.28	0.04	-0.13
	$^1L_8$	$^3M_8$	$^3M_9(16)$		
16			0.04±0.11		
19			0.10±0.12		
OPE	0.10	0.02	-0.10		

for *N*=13 are compared to the data in Figs. 2-9; their individual contributions to  $\chi^2$  are displayed in Table IX. A striking result is the (statistically) too good fit to the *R*( $\theta$ ) data, line 4 in Table IX. The Rochester group<sup>7</sup> could find no reason to suspect that the quoted experimental errors on *R*( $\theta$ ) could be too large by the required factor of two; one should therefore probably view the low  $\chi^2$  as mainly accidental.<sup>14</sup>

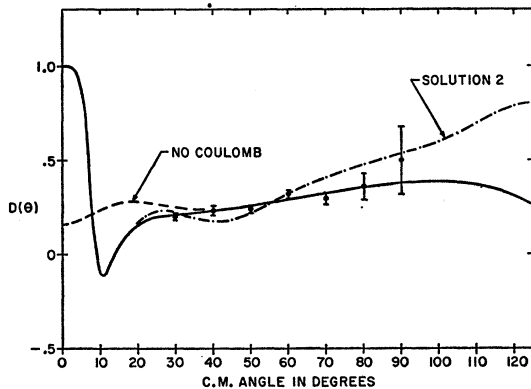


FIG. 4. The depolarization data. Notation as in Fig. 2. Note the large-angle difference in the two solutions.

<sup>14</sup> Modified phase-shift analyses of the 18.2-MeV Princeton and Saclay data (Ref. 3, pp. 92 and 180) give an interesting result which is clearly accidental. With 10 data and 4 free phases, one finds a  $\chi^2$  ratio of 0.06.

V. OTHER MODELS

Table X compares the phase shifts from the Yale phase-shift representations<sup>15</sup> YLAM and YRBI, the Saylor-Bryan-Marshak<sup>16</sup> (SBM) and Feshbach-Lomon-Tubis<sup>17</sup> (FLT II) boundary-condition-plus-potential models, the Hamada-Johnston<sup>13</sup> (HJ) potential and the Scotti-Wong<sup>18</sup> (SW) resonant boson exchange model.

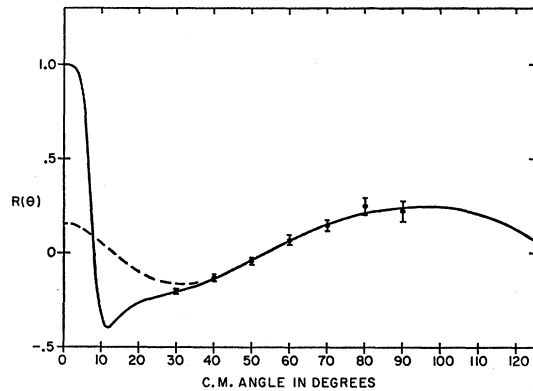


FIG. 5. The rotation data. Notation as in Fig. 2. Note the too-good fit to the data.

<sup>15</sup> G. Breit, M. H. Hull, Jr., K. E. Lassila, and K. D. Pyatt, Jr., Phys. Rev. **110**, 2227 (1960).

<sup>16</sup> D. P. Saylor, R. A. Bryan, and R. E. Marshak, Phys. Rev. Letters **5**, 266 (1960).

<sup>17</sup> E. L. Lomon, H. Feshbach, and A. Tubis, Bull. Am. Phys. Soc. **9**, 27 (1964); E. Lomon (private communication).

<sup>18</sup> A. Scotti and D. Y. Wong, Phys. Rev. Letters **10**, 142 (1963).

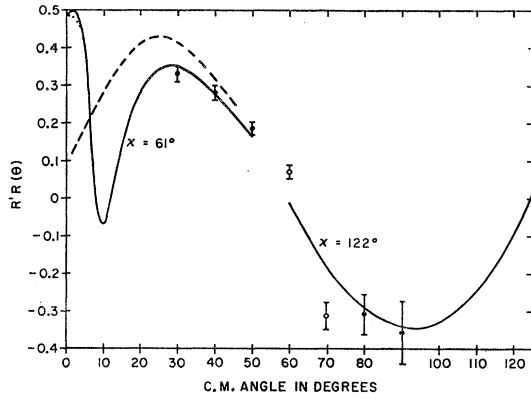


FIG. 6. The parameter  $R'R = R' \sin \chi + R \cos \chi$ , where  $\chi$  is a spin precession angle. Notation as in Fig. 2. The two data used in preliminary analyses only are shown as open circles.

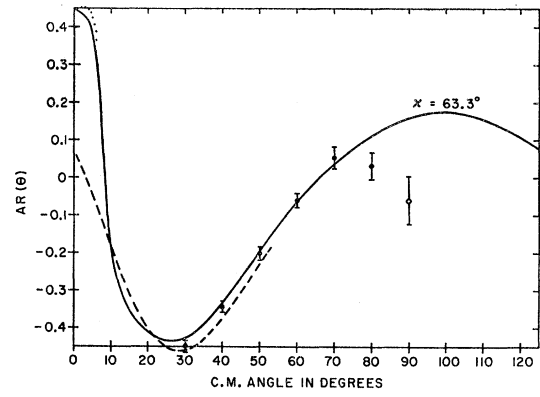


FIG. 7. The parameter  $AR = A \sin \chi + R \cos \chi$ , where  $\chi$  is a spin precession angle. Notation as in Fig. 6. Note that the 80 and 90° data might seem to be affected by an unsuspected experimental error which increases with angle.

The phases for the models were obtained as previously.<sup>8</sup>

The quantitative fit of each of the models to the 40 data is shown in Table XI. Release of the  $^1S_0$  from its

model value resulted in a significantly improved fit only for YRBI, the Yale potential, and FLT II. Both here

TABLE IX. Contributions of the individual data to  $\chi^2$ , for  $N=13$ . For 40 data with 27 degrees of freedom, the expected average contribution per datum is 0.675.

Data	c.m. Angles							Total	Fraction of expected average per datum
	30°	40°	50°	60°	70°	80°	90°		
$\sigma_{rel}$	0.46	0.61	0.07	0.71	0.12	0.43	0.46	2.86	0.61
$P_{rel}$	0.08	0.27	1.09	0.03	0.23	0.03	...	1.73	0.43
$D$	0.21	0.10	0.90	1.39	1.00	0.00	0.44	4.04	0.86
$R$	0.12	0.11	0.03	0.01	0.11	0.60	0.20	1.18	0.25
$AR$	2.12	0.31	0.18	0.04	0.21	5.07	...	7.93	1.96
$R'R$	0.84	0.00	2.94	...	...	0.10	0.60	4.48	1.33
$\sigma(90^\circ)$								0.13	0.19
$N_p$								0.44	0.65

TABLE X. Comparison of phase shifts from various models (see text). The values are nuclear bar, in degrees.

Model	$^1S_0$	$^3P_0$	$^3P_1$	$^3P_2$	$\epsilon_2$	$^1D_2$	$^3F_2$
YLAM	4.01	-2.01	-22.35	16.90	-2.41	7.91	0.49
YRBI	4.01	3.15	-22.92	15.47	-2.90	7.22	0.13
SBM	7.29	-0.48	-21.63	17.75	-2.55	7.73	1.66
HJ	5.09	-2.34	-20.95	17.43	-2.49	7.97	1.47
Yale	0.60	-2.04	-21.79	16.78	-2.39	8.62	0.84
SW	3.9	-1.1	-19.0	16.0	-3.0	8.2	0.65
FLT II	2.49	-0.96	-22.83	17.49	-2.74	8.15	2.15
OPE					-5.42	2.27	2.15
OPE(13)	$5.19 \pm 0.44$	$-1.37 \pm 0.58$	$-22.09 \pm 0.71$	$15.99 \pm 0.28$	$-2.85 \pm 0.19$	$7.13 \pm 0.29$	$1.49 \pm 0.37$
OPE II(13) <sup>a</sup>	$-11.67 \pm 0.85$	$-30.6 \pm 2.1$	$-4.01 \pm 0.42$	$18.12 \pm 0.63$	$-8.18 \pm 0.43$	$3.42 \pm 0.30$	$1.45 \pm 0.95$
Model	$^3F_3$	$^3F_4$	$\epsilon_4$	$^1G_4$	$^3H_4$	$^3H_5$	$^3H_6$
YLAM	-3.29	0.83	-1.20				
YRBI	-2.13	1.40	-0.76	0.74			
SBM	-3.18	0.99	-1.25	0.93	0.34	-0.90	0.16
HJ	-2.86	1.60	-1.18	0.95	0.48	-0.76	0.09
Yale	-3.49	1.16	-1.47	1.23	0.47	-1.04	0.26
SW	-2.77	1.93	-1.18	1.07	0.23		
FLT II	-3.01	1.37	-1.31	1.23	0.43	-0.93	0.24
OPE	-3.66	0.65	-1.25	0.75	0.37	-0.93	0.15
OPE(13)	$-2.62 \pm 0.21$	$2.25 \pm 0.20$	$-1.03 \pm 0.09$	$1.12 \pm 0.14$		$-0.64 \pm 0.18$	$0.35 \pm 0.09$
OPE II(13) <sup>a</sup>	$-1.98 \pm 0.25$	$1.55 \pm 0.55$	$-1.42 \pm 0.27$	$1.85 \pm 0.24$		$-0.64 \pm 0.18$	$0.35 \pm 0.09$

<sup>a</sup> Solution 2.

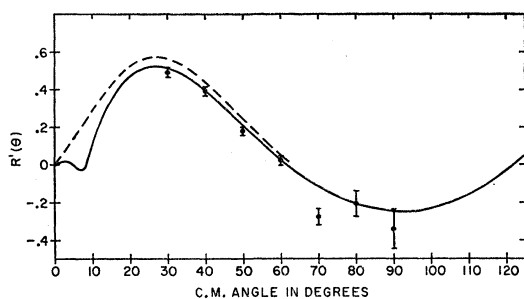


FIG. 8. The  $R'$  data deduced from  $R'R$  and  $R$ . Notation as in Fig. 2. These data were not used in the analyses.

and at 142 MeV,<sup>19</sup> release of the  $^1S_0$  resulted in a drop in  $\chi^2$  by about  $\frac{1}{3}$  for YLAM. The Yale potential  $\chi^2$  dropped from 263 to 156 upon release of the  $^1S_0$ , and the FLT II  $\chi^2$  dropped from 379 to 196. Either these models had not achieved a least squares fit to the data, or the behavior

TABLE XI. Goodness of fit of various models to the 40 data at 213 MeV.

Model	$\chi^2$	$\chi^2/\chi^2[\text{OPE}(13)]$	Remarks
YLAM	143	6.3	$R'R(50^\circ)$ too positive
YRBI	305	13.4	$P(60^\circ)$ too small; $\sigma$ , $P$ , $R'R$ , $AR$ off at forward angles
SBM	287	12.6	$R'R(40-50^\circ)$ too positive, $A(50-60^\circ)$ too negative, $P(30^\circ)$ too small
HJ	197	8.6	$R'R(30-50^\circ)$ too positive, $AR(40-50^\circ)$ too negative
Yale	263	11.5	$R$ too positive
SW	371	16.3	$D(30^\circ)$ too positive; $\sigma$ , $P$ , $R'R$ , $AR$ off at forward angles
FLT II	379	16.6	$\sigma$ , $P$ , $D$ , $R$ , $AR$ off at forward angles, $\sigma$ off near $90^\circ$
OPE(13)	22.8		

TABLE XII. Fractional increases in the phase-shift standard deviations upon the removal of data subgroups from the basic 40-piece data set. For example, removal of all of the  $D(\theta)$  data and reminimization of  $\chi^2$  yielded  $^1S_0 = 4.95 \pm 0.59$ , compared to  $^1S_0 = 5.19 \pm 0.44$  with the full 40-piece data set.

Phase	$\sigma_{\text{rel}}$	$\sigma(90^\circ)$	$P$	$N_p$	$D$	$R$	$AR$	$R'R$	$AR(80^\circ)$
$^1S_0$	1.27	0.07	0.14	-0.03	0.34	2.73	-0.30	0.11	-0.12
$^1D_2$	1.93	0.48	0.10	-0.04	0.10	0.62	-0.29	0.00	-0.14
$^1G_4$	1.29	0.07	0.07	0.00	0.07	1.57	-0.21	0.00	-0.16
$^3P_0$	0.12	0.46	0.00	-0.06	3.34	0.19	-0.32	0.07	-0.15
$^3F_2$	0.38	0.68	0.51	0.13	1.24	0.35	-0.22	0.08	-0.14
$^3P_1$	1.84	1.07	-0.04	-0.04	0.08	0.18	-0.22	0.01	-0.15
$^3F_3$	1.76	0.38	0.14	-0.05	0.38	2.24	0.19	0.00	-0.14
$^3H_6$	0.22	0.11	0.22	0.00	0.06	1.00	0.50	0.06	-0.11
$^3P_2$	1.64	0.68	0.68	0.18	0.25	0.28	-0.08	0.00	-0.15
$^3F_4$	3.60	0.55	0.60	0.05	0.55	0.50	-0.35	0.15	-0.15
$^3H_6$	4.00	0.00	0.00	0.00	0.11	0.00	-0.22	0.00	-0.22
$\epsilon_2$	0.47	0.79	0.42	-0.06	1.26	0.05	-0.26	0.00	-0.16
$\epsilon_4$	2.00	0.11	0.11	0.00	1.11	0.33	-0.22	0.00	-0.21

<sup>19</sup> P. Signell and D. Marker, Phys. Rev. 134, B365 (1964).

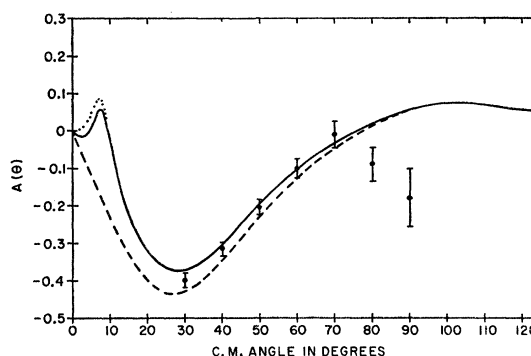


FIG. 9. The  $A$  data deduced from  $AR$  and  $R$ . Notation as in Fig. 2. These data were not used in the analyses.

of the  $^1S_0$  phase shift is more complex than is allowed by the model parameterizations.

## VI. SENSITIVITY TO DATA SUBGROUPS

The relative influence of the various data subgroups has been estimated by removing individual subgroups and then reminimizing  $\chi^2$ . The resulting fractional increases in the phase shift standard deviations are shown in Table XII; normalized shifts in the phases themselves are displayed in Table XIII. The two tables indicate that the results of the phase-shift analysis are most insensitive to  $R'R$  and  $N_p$ . New experiments aimed at moderately improving those data would seem to be least likely to produce significant results.

Although the  $AR(80^\circ)$  has the largest single-datum contribution to  $\chi^2$  (Table IX), its removal has only a small effect on the phases and their standard deviations when compared to the effect of removing all  $AR(\theta)$  data (Tables XII, XIII, and XIV). The large changes in the values of some of the phase shifts in the  $AR$  column of



TABLE XIII. Changes in the phase shifts upon the removal of data subgroups from the basic 40-piece data set. The values have been divided by the sum of the initial and final standard deviations. For an example, see the Table XII caption.

Phase	$\sigma_{rel}$	$\sigma(90^\circ)$	$P$	$N_p$	$D$	$R$	$AR$	$R'R$	$AR(80^\circ)$
$^1S_0$	-0.23	-0.10	-0.55	-0.02	-0.23	0.77	-0.52	0.38	-0.23
$^1D_2$	-0.22	-0.25	-0.56	-0.07	-0.07	0.57	-0.42	-0.05	0.04
$^1G_4$	0.02	-0.10	0.17	0.14	0.17	-0.64	-0.52	0.07	-0.27
$^3D_0$	0.24	0.21	-0.62	-0.10	-1.00	0.00	0.15	0.38	-0.09
$^3F_2$	0.24	-0.23	1.02	0.33	0.30	-0.44	-0.92	-0.25	-0.03
$^3D_1$	0.30	0.32	-0.02	0.09	0.09	-0.25	-1.19	0.14	-0.11
$^3F_3$	0.14	0.20	-0.60	-0.07	-0.24	0.61	1.89	0.17	0.05
$^3H_5$	-0.08	0.11	-0.55	-0.19	-0.08	0.69	-2.02	-0.11	-0.35
$^3D_2$	-0.26	-0.28	-1.11	-0.38	-0.06	-0.42	-1.22	0.20	-0.10
$^3F_4$	-0.02	-0.20	1.15	0.29	0.37	-0.24	-0.24	-0.26	-0.05
$^3H_6$	0.80	0.06	0.06	-0.17	0.11	0.00	-1.44	-0.17	-0.19
$\epsilon_2$	0.38	0.28	-0.85	-0.14	0.26	0.08	0.61	0.05	0.00
$\epsilon_4$	0.72	0.11	0.11	-0.06	-0.11	0.00	-0.44	0.00	-0.18

TABLE XIV.  $\chi^2$  ratio upon the removal of data subgroups and reminimization for  $N=13$ .

Solution No.	Data subgroup removed									
	None	$\sigma_{rel}$	$\sigma(90^\circ)$	$P$	$N_p$	$D$	$R$	$AR$	$R'R$	$AR(80^\circ)$
1	0.85	0.91	0.86	0.86	0.83	0.87	0.96	0.39	0.77	0.64
2	2.18	1.26	2.23	2.01	2.19	1.08	2.60	1.32	2.48	1.66

Table XIII are somewhat distressing. Experiments to remeasure  $AR$  in the range  $80-120^\circ$  are currently in progress at Rochester; it would also seem of interest to check  $AR$  at the lower angles.

### VII. SOLUTION 2

The low angular momentum phase shifts considered in the previous sections have all been of the type labeled No. 1 by Stapp, Ypsilantis, and Metropolis<sup>20</sup> (SYM). Of the six main solutions found by SYM, No. 1 is strongly favored by the data at  $50^\circ$ ,<sup>21</sup>  $142^\circ$ ,<sup>19</sup> and  $213^\circ$  MeV. The next most probable is that labeled No. 2 by SYM.

The results of using  $N=13$  and solution 2 low angular momentum phases with the current 40-piece data set are shown in Tables X, XIV, and XV. For a reasonable number  $N$  of searched upon phases, the  $\chi^2$  probability ( $P_q$  in Table XV) is less than 1%. Even with the removal of the somewhat uncertain  $AR$  data, the  $\chi^2$  probability is only 14% for this solution. If one multiplies the  $\chi^2$  for both solutions without  $AR$  by a number such that the solution 1  $\chi^2$  probability is 50%, then the solution 2 probability is again less than 1%. Comparing the two rows of Table IX, it is obvious that the separation is mainly due to  $\sigma_{rel}$  and  $D$ ; withdrawal of either one

of them drastically reduces the difference in  $\chi^2$  of the two solutions.

TABLE XV. As in Table V, but with the low angular momentum phases of the type labeled solution 2 by SYM (see text and Table X).

$N$	Phase	$\chi^2$	$M$	$\chi^2$ Ratio	$P_q$	$P_F$
5	$^1D_2$	459.	35	13.1		
6	$^3F_4$	261.	34	7.68		
7	$^3F_3$	149.	33	4.53		
8	$\epsilon_2$	115.	32	3.60		
9	$^1G_4$	74.1	31	2.39		0.00
10	$\epsilon_4$	69.6	30	2.32		0.16
11	$\epsilon_6$	64.1	29	2.21		0.11
12	$\epsilon_8$	61.2	28	2.18		0.25
13	$^3F_2$	58.9	27	2.18		0.30
14	$^3H_4$	56.5	26	2.17		0.30
15	$^3K_6$	53.4	25	2.14		0.22
16	$^3H_5$	46.5	24	1.94	<0.01	0.06
17	$^3K_7$	30.4	23	1.32	0.14	0.00
18	$^3M_9$	28.0	22	1.27	0.18	0.16
19	$^3M_8$	26.9	21	1.28	0.17	0.37
20	$^1I_6$	26.6	20	1.33	0.15	0.62
21	$^1L_8$	25.1	19	1.32	0.16	0.28

### VIII. THE PION-NUCLEON COUPLING CONSTANT

In the usual manner,<sup>19</sup> one can try to obtain evidence for the one-pion-exchange mechanism by allowing the pion-nucleon coupling constant  $g^2$  to be a free parameter. Table XVI displays the result, using the statistical ordering procedure outlined in Sec. IIIB. As in the case where  $g^2$  was fixed at the pion-nucleon value (Table V),

<sup>20</sup> H. P. Stapp, T. J. Ypsilantis, and N. Metropolis, Phys. Rev. **105**, 302 (1957).

<sup>21</sup> C. J. Batty and R. S. Gilmore, Rutherford High Energy Laboratory PLA Progress Report, 1963, pp. 80-83 (unpublished), and P. Signell (to be published).

TABLE XVI. As in Table V, but with the pion-nucleon coupling constant  $g^2$  as a free (searched-upon) parameter.

$N-1$	Phase	$\chi^2$	$M$	$\chi^2$ Ratio	$P_q$	$P_F$	$g^2$
6	${}^3F_4$	84.0	33	2.55	0.00		
7	$\epsilon_2$	52.2	32	1.63	0.01		
8	${}^1G_4$	34.4	31	1.11	0.32	0.00	$10.35 \pm 0.88$
9	${}^3H_6$	26.7	30	0.890	0.65	0.00	$10.69 \pm 0.80$
10	${}^3F_3$	25.9	29	0.894	0.64	0.35	$11.6 \pm 1.3$
11	${}^3H_5$	25.5	28	0.911	0.61	0.49	$11.8 \pm 1.4$
12	${}^3K_7$	20.8	27	0.771	0.80	0.01	$11.2 \pm 1.2$
13	${}^3K_8$	19.0	26	0.729	0.84	0.11	$11.1 \pm 1.2$
14	${}^3F_2$	17.9	25	0.717	0.84	0.23	$11.9 \pm 1.4$
15	${}^3M_3$	17.3	24	0.721	0.84	0.35	$12.5 \pm 1.5$
16	$\epsilon_4$	15.9	23	0.693	0.86	0.16	$18.8 \pm 4.9$
17	$\epsilon_6$	15.8	22	0.719	0.82	0.67	$15 \pm 10$
18	${}^3H_4$	15.7	21	0.746	0.79	0.66	$11 \pm 13$
19	${}^3K_6$	14.6	20	0.729	0.80	0.22	$8 \pm 13$
20	${}^1I_6$	14.3	19	0.752	0.77	0.53	$1 \pm 18$
21	${}^1L_8$	13.6	18	0.757	0.76	0.35	$-11 \pm 25$

the  $F$  probabilities do not rise to a high level and then stay there. Even at  $N=20$  and  $22$ , one finds the probability dipping back down.

In contrast to Table V, here, one should, strictly speaking, no longer use departures of higher  $L$  phases from OPE as criteria for stopping at a particular  $N$ . If we do anyway, and take the preferred fixed- $g^2$  value of  $N=13$ , then the predicted  $g^2$  is  $11.1 \pm 1.2$  with  $\chi^2=19.0$ . The order of release of the phases, displayed in Table XVI, is not at all like the believable pattern shown earlier for fixed  $g^2$ . In fact, the eleventh, twelfth, and thirteenth released phases all have the same  $L$ -to- $J$  relationship. In this case one naturally wonders about the values which would be obtained with a different set of released phases. To examine this, we searched on the same 13 phases as in the preferred fixed- $g^2$  analysis. With  $g^2$  also a free parameter so that  $N=14$ , the minimized  $\chi^2$  was 21.3 and  $g^2=18.8 \pm 3.5$ . As at 142 MeV,<sup>19</sup> then, the evidence for the one-pion exchange mechanism can only be considered qualitative.

### IX. THE HIGHER $L$ PHASES

The preferred analysis has been that for which 13 of the lower angular momentum phases were free, and the rest were at their OPE values. In actuality, of course, the higher  $L$  phases contain multipion-exchange contributions.

The basic assumption of the modified phase-shift analysis is that for higher  $L$  the multipion effects are negligible compared to the OPE contributions. We have examined this assumption by remaking the  $N=13$  analysis with two different models for the higher  $L$  phases. First, the Hamada-Johnston potential<sup>12</sup> was used for the higher  $L$  phases and  $\chi^2$  was reminimized; no phase-shift standard deviation changed significantly, and only one phase-shift value changed by an appreciable fraction of its associated standard deviation. That was the  ${}^3H_6$ , which went from  $0.35^\circ \pm 0.09$  (Table VIII)

to  $0.40^\circ \pm 0.09$ . Next, the "ALV3+ $\omega$ " model<sup>22</sup> was used for the higher  $L$  phases. This model contains scalar,  $\rho$ , and  $\omega$  mesons, and the "2 $\pi$  basic"  $N\bar{N} \rightarrow 2\pi L \geq 2$  contributions computed by Amati, Leader, and Vitale.<sup>23</sup> After  $\chi^2$  had been reminimized, it was found that no phase shift or its standard deviation had changed by more than 10% of the standard deviation.

One concludes that the neglect of multipion contributions has little effect on the values and errors of the predicted low- $L$  phases.

### X. EXTENSIONS OF THE EXPERIMENTS

Experiments are being planned<sup>7</sup> for the extension of the data to lower and higher angles. It would be helpful if some guides could be found as to which measurements might be more productive.

From the discussion in Sec. VIII, it would appear that further discrimination against solution 2 could be sought by smaller angle cross section or higher angle depolarization measurements. To obtain an indication of the effect of such measurements, hypothetical data of each kind were added in turn to the 40 actual data. First, the predicted cross section values at 15, 20, and 25° (Fig. 2) were added to the data set, with assigned errors similar to those for the actual data at nearby angles (see Table XVIII). The solution 1 analysis was of course unaffected, but the solution 2 reminimized  $\chi^2$  was 71.7, compared to the actual-data value of 58.9. Then the predicted depolarization values at 100°, 110°, and 120° (Fig. 4) were added to the actual-data set, with assigned errors of 0.10 from estimates of experimental feasibility.<sup>7</sup> The reminimized  $\chi^2$  was 61.5, a negligible increase over the actual-data value. The conclusion would seem to be that extension of the measurements to nearby lower and higher angles will not substantially widen the  $\chi^2$  separation of the two solutions.

One can obtain estimates of reduction in phase-shift uncertainties in a manner similar to that described above for further separation of the solutions. Errors were assigned as above, and are shown in Table XVIII. The fractional decreases in the phase shift deviations for the various extensions are shown in Table XVII. Thus, for instance, if it becomes theoretically desirable to have the  ${}^1G_4$  further pinned down, then small angle cross sections would certainly be the measurement to make. On the other hand, if one needed substantial further delineation of  $\epsilon_4$ , a simple angular extension of the current measurements would not be likely to produce it. The effect of combined subgroup measurements has not been studied.

Golaskie and Palmieri<sup>24</sup> have recently obtained an absolute cross section measurement at 147 MeV to

<sup>22</sup> J. Durso and P. Signell, Phys. Rev. **135**, B1057 (1964).

<sup>23</sup> D. Amati, E. Leader, and B. Vitale, Phys. Rev. **130**, 750 (1963).

<sup>24</sup> R. Golaskie and J. N. Palmieri, Harvard Cyclotron Laboratory (to be published).

TABLE XVII. Fractional decreases in the phase-shift standard deviations with hypothetical data added to the 40 actual data. The values of the added data were those predicted by the  $N=13$  preferred analysis (Figs. 2-9). The errors assigned them were as in Table XVIII.

Phase shift	$\sigma_{\text{abs}}(90^\circ)$	$\sigma$	$P$	15°, 20°, 25°		$AR$	$R'R$	$D$	100°, 110°, 120°		
				$D$	$R$				$R$	$AR$	$R'R$
$^1S_0$	0.05	0.13	0.16	0.05	0.06	0.06	0.05	0.06	0.17	0.14	0.11
$^1D_2$	0.25	0.25	0.23	0.10	0.20	0.10	0.09	0.06	0.10	0.11	0.08
$^1G_4$	0.09	0.43	0.26	0.06	0.07	0.06	0.05	0.05	0.09	0.07	0.07
$^3P_0$	0.20	0.07	0.06	0.07	0.09	0.07	0.07	0.09	0.06	0.07	0.06
$^3F_2$	0.22	0.14	0.08	0.07	0.13	0.15	0.07	0.07	0.06	0.08	0.06
$^3P_1$	0.65	0.16	0.13	0.06	0.08	0.28	0.11	0.05	0.07	0.07	0.05
$^3F_3$	0.15	0.10	0.07	0.08	0.10	0.09	0.13	0.06	0.09	0.14	0.07
$^3H_5$	0.04	0.11	0.09	0.23	0.33	0.08	0.37	0.06	0.13	0.20	0.08
$^3P_2$	0.35	0.12	0.09	0.14	0.24	0.12	0.11	0.06	0.06	0.08	0.06
$^3F_4$	0.15	0.15	0.05	0.06	0.16	0.13	0.09	0.05	0.05	0.06	0.06
$^3H_6$	0.10	0.15	0.25	0.18	0.11	0.14	0.18	0.07	0.07	0.10	0.06
$\epsilon_2$	0.25	0.15	0.11	0.06	0.08	0.16	0.08	0.05	0.07	0.06	0.05
$\epsilon_4$	0.05	0.08	0.07	0.22	0.11	0.07	0.07	0.08	0.05	0.05	0.05

better than 1%. The effect of a similar measurement at 213 MeV was estimated by adding a hypothetical  $\sigma(90^\circ)$  datum, with results as in Table XVII. Notice that the error on the  $^3P_1$  was reduced to 35% of its former value. Roughly, the effect is proportional to the magnitude of the phase shift, as one would expect.

TABLE XVIII. Standard deviations assigned (see text) to the hypothetical data of Table XVII.  $\sigma_{\text{abs}}(90^\circ) = 3.65 \pm 0.03$ .

c.m. Angles	$\sigma$	$P$	$D$	$R$	$AR$	$R'R$
15°, 20°, 25°	0.050	0.006	0.016	0.012	0.016	0.020
100°, 110°, 120°			0.10	0.040	0.040	0.08

## XI. SUMMARY

With one interpolated and 42 measured data, preliminary analyses and statistical arguments led to the discarding of three data.

Standard "modified phase-shift analyses" with a statistical order of release of the phase shifts resulted in the eventual choice of thirteen free low angular momentum phase shifts. The  $\chi^2$  probabilities were ambiguous, and the  $F$  probabilities were rejected as probably unphysical. Most of the 13 free phases had very small uncertainties (standard deviations).

Several of the data subgroups had unexpectedly low contributions to  $\chi^2$ , but no apparent cause was found.

A number of proton-proton models were compared to the data; the fits were generally poor,  $\chi^2$  being an order of magnitude larger than for the modified phase-shift analysis results. Release of the  $^1S_0$  phase still did not make any of the models into a statistically good fit.

The small  $\chi^2$  probability for solution 2 was found to be due mainly to the relative cross section and to  $D(\theta)$ .

Only very rough correspondence could be established between the value of the pion-nucleon coupling constant obtained from the 213-MeV proton-proton data, and that obtained from pion-nucleon phenomena.

## ACKNOWLEDGMENTS

We wish to thank K. Gotow, F. Lobkowicz, J. Tinlot, and R. Warner for very helpful discussions concerning the data. We are much indebted to B. Rose for persuading us to put data rejection on a statistical basis whenever possible. One of us (J. E. M.) gratefully acknowledges the assistance of a National Science Foundation Research Participation Grant. The calculations reported here were carried out in the Computation Center of The Pennsylvania State University and in the A. E. C. Computation Center at New York University.